AIAA 2001-0162
Estimating Bias Error Distributions

Tianshu Liu and Tom D. Finley

NASA Langley Research Center
Hampton, VA 23681-2199

39th AIAA Aerospace Sciences
Meeting & Exhibit
8-11 January 2001 / Reno, NV

AIAA 2001-0162

Estimating Bias Error Distributions

Tianshu Liu† and Tom D. Finley†
NASA Langley Research Center
Hampton, VA 23681-2199

Abstract

This paper formulates the general methodology for estimating the bias error distribution of a device in a measuring domain from less accurate measurements when a minimal number of standard values (typically two values) are available. A new perspective is that the bias error distribution can be found as a solution of an intrinsic functional equation in a domain. Based on this theory, the scaling- and translation-based methods for determining the bias error distribution are developed. These methods are virtually applicable to any device as long as the bias error distribution of the device can be sufficiently described by a power series (a polynomial) or a Fourier series in a domain. These methods have been validated through computational simulations and laboratory calibration experiments for a number of different devices.

1. Introduction

The measurement of an instrument always has error defined as the difference between the measured value and the true value. The total error is the sum of the bias error and the random error. Most books and articles on uncertainty analysis have studied in detail statistical estimates of the random error [1,2]. However, the bias error, which is the fixed, systematic component of the total error, is not sufficiently discussed because it is often assumed that all bias errors have been eliminated by calibration. Indeed, the bias error can be determined by comparison with a standard having accuracy much better than the device being tested. The standard device is ultimately traceable to a national or international standard laboratory. If the standard values over the whole range of measurements are known, the determination of the bias error distribution of an instrument is extremely trivial. Unfortunately, it is not always possible to have a standard device available for calibration. Also, the standard device itself has limited accuracy. Finley [3] proposed a unique idea for extracting the absolute bias error of an angular measurement device by comparing it with another instrument of comparable quality. The differences in readings from the two devices are obtained with two different initial angles of the devices. Next, a Fourier analysis of the two sets of the differences recovered the bias errors for both devices. Finley's method was further discussed by Snow [4] from the standpoint of the Fourier transform. Finley's work shows that in angular measurements the absolute bias error distributions can be obtained by using two less accurate devices. Naturally, a legitimate question is whether there is a general method for estimating the bias error distribution of a device. This question will be answered in this paper.

This paper formulates the general methodology for estimating the absolute bias error distribution of a device in a measuring domain when only a few standard values (typically two values) are known. In the proposed approach, the bias error distribution is sought as a solution of an intrinsic functional equation in a measuring domain. The scaling-based method and translation-based method are developed, in which the analytical solutions to the functional equations for the bias error distributions are, respectively, expressed as a power series and a Fourier series in a given domain. The scaling-based method is effective for a large class of the bias error distributions that can be sufficiently described by a power series or a polynomial. The approximate scaling-based method for practical implementation is developed, requiring two standard values to determine the complete bias error distribution. An empirical rule for selecting an appropriate order of a polynomial is suggested to achieve the good accuracy of calculating the bias error distribution. Effects of the random measurement perturbations on calculation of the bias error distribution are studied through Monte Carlo simulations. In contrast to the scaling-based method, the translation-based method has relatively limited applications, but it is particularly useful for angular measurements since the bias error distribution can be naturally expressed as a Fourier series. The scaling- and translation-based methods for simultaneously estimating the bias error distributions of two devices are also described. Computational simulations and laboratory experiments for calibrating a number of different devices are conducted to validate the proposed methodology to recover the bias error distribution.

2. Bias Error and Intrinsic Functional Equation

Let $m(x)$ be the measurement value of a 'true' physical quantity x by a device having a deterministic bias error $\varepsilon(x)$ then,

† Research Scientist, Model Systems Branch, Member AIAA

$$m(x) = x + \varepsilon(x). \quad (1)$$

The symbol $m(x)$ can be interpreted as a measurement operator of the variable x. In order to obtain an additional independent equation for $\varepsilon(x)$, a quantity $\alpha x + \beta$ that is a linear transformation of x is measured by the same device, where α is a scaling constant and β is a translation constant. The measurement value of $\alpha x + \beta$ is expressed as

$$m(\alpha x + \beta) = \alpha x + \beta + \varepsilon(\alpha x + \beta). \quad (2)$$

Eliminating x in Eqs. (1) and (2), one obtains a functional equation for $\varepsilon(x)$

$$\delta(x) = \varepsilon(x) - \alpha^{-1}\varepsilon(\alpha x + \beta), \quad (3)$$

where the difference $\delta(x)$ is a known function that can be measured by the device for given α and β, i.e.,

$$\delta(x) = m(x) - \alpha^{-1}(m(\alpha x + \beta) - \beta). \quad (4)$$

Eq. (3) is an intrinsic functional equation governing the bias error distribution $\varepsilon(x)$. Because no assumption has been made, this functional equation for the bias error distribution is virtually applicable to any measurement instrument. Although more complicated functional equations can be similarly constructed as a model of the bias error, Eq. (3) enjoys its simplicity without loss of generality. Now, the fundamental problem is to find a solution to Eq. (3) for $\varepsilon(x)$ in a given domain $D = [x_1, x_2]$ and a class of admissible functions (including domains and ranges). The discussions on functional equations from a mathematical perspective can be found in references 5 and 6. Although a general solution to Eq. (3) in the power-series-form can be found, two special but very useful cases are considered here, which are a pure scaling case ($\alpha \neq 0, 1$ and $\beta = 0$) and a pure translation case ($\alpha = 1$ and $\beta \neq 0$). Not only the special cases lead to simpler solutions, but also they are more easily implemented in the real measurements.

The Scaling-Based Method

In the pure scaling case ($\alpha \neq 0, 1$ and $\beta = 0$), the intrinsic functional equation is

$$\delta(x) = \varepsilon(x) - \alpha^{-1}\varepsilon(\alpha x), \quad (5)$$

where $\delta(x)$ is a known function

$$\delta(x) = m(x) - \alpha^{-1} m(\alpha x). \quad (6)$$

Assume that the functions $\delta(x)$ and $\varepsilon(x)$ can be expanded as a power series in a given domain $D = [x_1, x_2]$, that is,

$$\delta(x) = \sum_{n=0}^{N} d_n x^n \text{ and } \varepsilon(x) = \sum_{n=0}^{N} e_n x^n. \quad (7)$$

For a given set of measurement data points of $\delta(x)$, the coefficients d_n can be obtained using the least-squares method (see Appendix). Substituting Eq. (7) into Eq. (5), one can determine all the coefficients e_n except for $n = 1$,

$$e_n = d_n / (1 - \alpha^{n-1}). \quad (n = 0, 2, 3 \cdots N) \quad (8)$$

For $n = 1$, to determine the remaining unknown coefficient e_1, the measurement value $m(x)$ is re-written as

$$m(x) = \sum_{\substack{n=0 \\ n \neq 1}}^{N} e_n x^n + (1 + e_1) x. \quad (9)$$

Integrating Eq. (9) over a given domain $D_s = [x_{1s}, x_{2s}] \subseteq D = [x_1, x_2]$, one obtains an expression for the coefficient e_1

$$e_1 = \frac{2}{x_{2s}^2 - x_{1s}^2} \int_{x_{1s}}^{x_{2s}} [m(x) - \sum_{\substack{n=0 \\ n \neq 1}}^{N} e_n x^n] \, dx - 1, \quad (10)$$

where a condition $x_{1s}^2 \neq x_{2s}^2$ must hold. We often assign $[x_{1s}, x_{2s}] = [x_1, x_2]$ if $x_1^2 \neq x_2^2$. Thus, all the coefficients e_n are obtained and the bias error distribution $\varepsilon(x)$ is, in principle, determined. Naturally, the above method is called as the scaling-based method for recovering the bias error.

An underlying assumption for the scaling-based method is that the functions $\delta(x)$ and $\varepsilon(x)$ can be sufficiently expressed as a power series or a polynomial in $D = [x_1, x_2]$. To illustrate this method, we consider a hypothetical bias error distribution of a device in $D = [1, 10]$,

$$\varepsilon(x) = 0.3 - 0.01\sqrt{x} + 0.03x - 4 \times 10^{-4} x^2 - 10^{-4} x^3 - 6 \times 10^{-6} x^5 + 0.5 \exp(-0.3x^2). \quad (11)$$

As shown in Fig. 1, the bias error distribution computed by using the scaling-based method for $\alpha = 2$ and $N = 13$ is in excellent agreement with one given by Eq. (11). The difference between the given and computed bias errors is also plotted in Fig. 1.

In an ideal case, it seems likely to recover the bias error distribution even without using any standard value. However, one may notice that both $\delta(x)$ and $\varepsilon(x)$ in Eq. (7) are expanded as a function of the true variable x which is not exactly known *a priori*. It will be pointed out later that the approximate scaling-based method for actual measurements still needs two standard values to recover the bias error distribution in the domain $D = [x_1, x_2]$.

The Translation-Based Method

In the pure translation case ($\alpha = 1$ and $\beta \neq 0$), instead of using a power series, a Fourier series is employed because of the shift property of a complex exponential function. Since a Fourier series has the periodic property, the variable x and the translation

constant β in Eqs. (3) and (4) are replaced by the angular variables θ and θ_0, respectively. In a domain $D_\theta = [0, 2\pi]$, the intrinsic functional equation for the bias error distribution $\varepsilon(\theta)$ is

$$\delta(\theta) = \varepsilon(\theta) - \varepsilon(\theta + \theta_0), \quad (12)$$

where $\delta(\theta)$ is a known function for a given θ_0

$$\delta(\theta) = m(\theta) - m(\theta + \theta_0) + \theta_0. \quad (13)$$

Assume that the functions $\delta(\theta)$ and $\varepsilon(\theta)$ in $D_\theta = [0, 2\pi]$ can be expanded as a Fourier series

$$\delta(\theta) = \sum_{n=1}^{N} [a_n^{(\delta)} \cos(n\theta) + b_n^{(\delta)} \sin(n\theta)],$$

$$\varepsilon(\theta) = a_0^{(\varepsilon)}/2 + \sum_{n=1}^{N} [a_n^{(\varepsilon)} \cos(n\theta) + b_n^{(\varepsilon)} \sin(n\theta)]. \quad (14)$$

The coefficients $a_n^{(\delta)}$ and $b_n^{(\delta)}$ in $\delta(\theta)$ can be determined using the least-squares method for a given set of data points (see Appendix). For $n \neq 0$, a relation between ($a_n^{(\varepsilon)}$, $b_n^{(\varepsilon)}$) and ($a_n^{(\delta)}$, $b_n^{(\delta)}$) $(n = 1, 2, \cdots N)$ is derived by substituting Eq. (14) into Eq. (12), that is,

$$\left(a_n^{(\varepsilon)}, b_n^{(\varepsilon)}\right)^T = G^{-1}\left(a_n^{(\delta)}, b_n^{(\delta)}\right)^T, \ (n = 1, 2, 3 \cdots N) \quad (15)$$

where

$$G = \begin{pmatrix} 1 - \cos(n\theta_0) & -\sin(n\theta_0) \\ \sin(n\theta_0) & 1 - \cos(n\theta_0) \end{pmatrix}.$$

Because the determinant $det(G) = 2[1 - \cos(n\theta_0)]$ should not be zero for the existence of a unique solution, the necessary conditions for a unique solution are $n\theta_0 \neq k\pi + \pi/2$ ($k = 0, 1, 2, \cdots$) and $n \neq 0$. For $n = 0$, similar to the pure scaling case, the coefficient $a_0^{(\varepsilon)}$ can be determined by the following integral over $D_\theta = [0, 2\pi]$

$$a_0^{(\varepsilon)} = \pi^{-1} \int_0^{2\pi} \{m(\theta) - \sum_{n=1}^{N} [a_n^{(\varepsilon)} \cos(n\theta) + b_n^{(\varepsilon)} \sin(n\theta)]\} d\theta - 2\pi. \quad (16)$$

Therefore, all the coefficients ($a_n^{(\varepsilon)}$, $b_n^{(\varepsilon)}$) are known and the bias error distribution $\varepsilon(\theta)$ is readily calculated. We refer to this method as the translation-based method. Note that the constant term in the Fourier series for $\delta(\theta)$ in Eq. (14) is zero. This is a restrictive assumption for the translation-based method. Another implicit assumption embedded in Eq. (14) is that the bias error distribution must be periodic.

As an example, consider a hypothetical bias error $\varepsilon(\theta)$ defined in $D_\theta = [0, 2\pi]$,

$$\varepsilon(\theta) = 0.08 + 0.02\cos(\theta) + 0.03\cos(2\theta) - 0.06\sin(2\theta) + 0.04\sqrt{\theta}\sin(4\theta). \quad (17)$$

Figure 2 shows a comparison between the given bias error distribution (17) and the distribution recovered by using the translation-based method ($\theta_0 = \pi/20$ and $N = 6$). Simulations indicate that the translation-based method is good for recovering the bias error distribution whose behavior is dominated by trigonometric functions. The Fourier series solution is particularly useful for angular measurements in the domain $D_\theta = [0, 2\pi]$. Compared to the scaling-based method, the translation-based method has limited applications because of the implicit assumption of periodicity $\theta(0) = \theta(2\pi)$. On the other hand, when the periodicity condition $\theta(0) = \theta(2\pi)$ is imbedded in data, the translation-based method does not explicitly require any standard value to recover the bias error distribution. In contrast, the scaling-based method typically needs two standard values in the real measurements (see Section 3).

3. The Approximate Scaling-Based Method

In Section 2, we describe the scaling-based method for recovering the bias error distribution as a solution of the functional equation. However, the method in the ideal condition cannot be directly applied to the real measurements because the true variable *x* in Eq. (7) is not known *a priori*. Therefore, an approximate approach is developed, in which the true variable *x* is replaced by a known approximate reference value x_{appr}. The approximate reference value x_{appr} is often a measurement value by another device with a comparable accuracy. Due to the substitution of x_{appr} for *x*, the scaling-based method gives an approximate bias error distribution $\varepsilon(x)_{appr}$ that deviates from the true bias error distribution $\varepsilon(x)$. The deviation of $\varepsilon(x)_{appr}$ from $\varepsilon(x)$ can be reasonably modeled by a linear function of x_{appr}. Thus, this approximate method requires two standard values to determine the unknown coefficients in the linear function of deviation for recovering the whole bias error distribution.

Replacing the true variable *x* in Eq. (7) by a known approximate reference variable x_{appr}, one obtains an alternative formulation

$$\delta(x)_{appr} = \sum_{n=0}^{N} d_n (x_{appr})^n$$

$$\varepsilon(x)_{appr} = \sum_{n=0}^{N} e_n (x_{appr})^n, \quad (18)$$

where the function $\delta(x)_{appr}$ is an approximate form of $\delta(x)$ in Eq. (6), i.e.,

$$\delta(x)_{appr} = m(x) - \alpha^{-1} m(\alpha x_{appr}). \quad (19)$$

The coefficients d_n can be obtained by using the least-squares method and the coefficients e_n are given by Eqs. (8) and (10) in Section 2. Therefore, the approximate bias error distribution $\varepsilon(x)_{appr}$ is determined.

Now, we estimate the difference between $\varepsilon(x)$ and $\varepsilon(x)_{appr}$. Assuming $x_{appr} = x + \varepsilon'(x)$, one knows

$$\begin{aligned} \varepsilon(x)_{appr} &= \sum_{n=0}^{N} e_n (x_{appr})^n \\ &= \varepsilon(x) + \sum_{n=1}^{N} n\, e_n \varepsilon'(x) x^{n-1} + o(\varepsilon') \end{aligned}, \tag{20}$$

where $\varepsilon'(x)$ is the bias error of the approximate reference value x_{appr} and $o(\varepsilon')$ is a higher-order small term of $\varepsilon'(x)$. Based on the triangle inequality and the Cauchy-Schwarz inequality, furthermore, one obtains the following estimate for the difference between $\varepsilon(x)$ and $\varepsilon(x)_{appr}$ in the domain $D = [x_1, x_2]$

$$\begin{aligned} &|| \varepsilon - \varepsilon_{appr} || / || \varepsilon || \\ &\le (|| \varepsilon' || / || \varepsilon ||) \sum_{n=1}^{N} n \left| e_n \right| \left(\frac{x_2^{2n-1} - x_1^{2n-1}}{2n-1} \right)^{1/2} + c \end{aligned}, \tag{21}$$

where c is a positive constant and $||\bullet||$ is the L_2-norm defined as $|| f || = [\int_{x_1}^{x_2} f^2(x)dx]^{1/2}$. Eq. (21) indicates that the upper bound of the norm $|| \varepsilon - \varepsilon_{appr} ||$ is simply proportional to $|| \varepsilon' || / || \varepsilon ||$, but it is related to the size of the domain $D = [x_1, x_2]$ in a non-linear fashion. Computational simulations indicate that $\varepsilon(x)_{appr}$ is often a shifted, rotated and sheared representation of $\varepsilon(x)$ although it describes the general behavior of $\varepsilon(x)$.

The difference between the true and approximate bias error distributions $\varepsilon(x)$ and $\varepsilon(x)_{appr}$ can be reasonably modeled by a linear function of x_{appr}, that is,

$$\varepsilon(x) = \varepsilon(x)_{appr} - (C_0 + C_1 x_{appr}). \tag{22}$$

The linear term serves as a correction for the approximate solution $\varepsilon(x)_{appr}$. Clearly, two standard values are required to determine the constants C_0 and C_1. When two true values are known at two specific points, the constants C_0 and C_1 can be determined. The linear model (22) is able to give a reasonable estimate for the bias error distribution. The approximate reference value x_{appr} is provided by another independent device with the accuracy comparable to the tested device.

As an example, consider a bias error distribution $\varepsilon(x)$ in $D = [1,10]$

$$\begin{aligned} \varepsilon(x) = 0.3 - 0.08\sqrt{x} - 8\times10^{-3} x^2 \\ + 8\times10^{-5} x^4 - exp(-0.3x^2) \end{aligned}. \tag{23}$$

The approximate reference value is given by $x_{appr} = x + \varepsilon'(x)$, where

$$\begin{aligned} \varepsilon'(x) = A[0.2 - 5\times10^{-3}\sqrt{x} + 0.02x^2 - 3\times10^{-3} x^3 \\ - 0.5\, exp(-0.2x) + 0.5\, sec\, h(0.18x)] \end{aligned}. \tag{24}$$

The constant A in Eq. (24) is used to adjust the magnitude of $\varepsilon'(x)$ in computational simulations. Figure 3 shows the given bias distribution (23) and the computed distributions for α = 2 and N = 13 when the relative magnitudes of $\varepsilon'(x)$ are $|| \varepsilon' || / || \varepsilon || = 0.29$, *1.17*, *1.75*, and *2.95*. As indicated in Fig. 3, the computed distribution is able to describe the behavior of the bias error distribution $\varepsilon(x)$ even when the accuracy of the approximate reference value is considerably worse than that of the tested device. Figure 4 shows the difference between the given and computed bias error distributions $|| \varepsilon(x) - \varepsilon(x)_{camp} || / || \varepsilon(x) ||$ as a function of $|| \varepsilon'(x) || / || \varepsilon(x) ||$. The linear relation between $|| \varepsilon(x) - \varepsilon(x)_{camp} || / || \varepsilon(x) ||$ and $|| \varepsilon'(x) || / || \varepsilon(x) ||$ shown in Fig. 4 is consistent with the theoretical estimate (21).

The selection of the order of the polynomial N in Eq. (18) significantly affects the accuracy in calculation of the bias error distribution. A polynomial having a low order may lead to a poor fit to the true values, while a polynomial having an excessively high order may produce a large variance due to the over-fitting problem. A question is whether there exists an optimal order of the polynomial to achieve the highest accuracy of calculation. An answer to this problem is not available in a strictly mathematical sense. Nevertheless, based on computational simulations for various bias error distributions, an empirical rule is proposed here for determining an appropriate order of the polynomial. We denote $\varepsilon(x, N)$ as the bias error distribution calculated using a *Nth*-order polynomial and define the norm $||\varepsilon(x, N+1) - \varepsilon(x, N)||$ as the distance between the bias error distributions calculated using the *(N+1)th*-order and *Nth*-order polynomials. Computational simulations show that the distance $||\varepsilon(x, N+1) - \varepsilon(x, N)||$ usually becomes small in a certain range of the order N when the polynomial correctly describes the true bias error distribution. This phenomenon can be clearly seen when $||\varepsilon(x, N+1) - \varepsilon(x, N)||$ is plotted as a function of the order N. Figure 5 shows a typical semi-logarithmic plot of $||\varepsilon(x, N+1) - \varepsilon(x, N)||$ as a function of the order N for

the given bias error distribution (23), indicating a characteristic valley in a range of N = 10-15. In this case, a polynomial having the order in N = 10-15 can provide a reasonable estimate for the bias error distribution.

4. Effects of Random Perturbations

In actual calibration experiments, a measurement $m(x)$ has the random error in addition to the bias error. The random error affects the solution of the intrinsic functional equation for recovering the bias error distribution. To simulate effects of the random perturbations, we consider a perturbed measurement $m(x)[1+p(x)]$, where $p(x)$ is a random perturbation with the normal distribution. Monte Carlo simulations can give the probability density distribution of the relative difference $||\tilde{\varepsilon}(x)-\varepsilon(x)||/||\varepsilon(x)||$ that is a random variable, where $\tilde{\varepsilon}(x)$ is the perturbed bias error distribution calculated by using the scaling-based method. For $p(x)$ having the standard deviation of 0.005, the scaling-based method with $\alpha = 2$ and N = 13 is used to recover the bias error distribution (11) for 500 samples. Figure 6 shows the probability density distribution of the relative difference $||\tilde{\varepsilon}(x)-\varepsilon(x)||/||\varepsilon(x)||$. The expectation value of $||\tilde{\varepsilon}(x)-\varepsilon(x)||/||\varepsilon(x)||$ is plotted in Fig. 7 as a function of the standard deviation of the random perturbation $p(x)$.

The scaling constant α may be also changed by a small random perturbation in certain measurements. The randomly perturbed scaling constant is expressed as $\alpha(1+p_\alpha)$, where p_α obeys the normal distribution. When p_α has the standard deviation of 0.005, the disturbed bias error distribution $\tilde{\varepsilon}(x)$ is calculated by using the scaling-based method ($\alpha = 2$ and N = 13) for 500 samples for the given bias error distribution (11). Figure 8 shows the resulting probability density distribution of $||\tilde{\varepsilon}(x)-\varepsilon(x)||/||\varepsilon(x)||$, indicating a roughly uniform distribution.

5. Methods for Simultaneously Estimating Bias Errors of Two Devices

The Scaling-Based Method

In this section, we describe the scaling-based method for simultaneously determining the bias error distributions of two devices. Consider devices A and B that have the measurements

$$m_A(x) = x + \varepsilon_A(x) \text{ and } m_B(x) = x + \varepsilon_B(x). \quad (25)$$

The intrinsic functional equations for the bias error distributions $\varepsilon_A(x)$ and $\varepsilon_B(x)$ are

$$\begin{aligned} \delta_1(x) &= \varepsilon_A(x) - \varepsilon_B(x) \\ \delta_2(x) &= \varepsilon_A(x) - \alpha^{-1}\varepsilon_B(\alpha x) \end{aligned}, \quad (26)$$

where $\delta_1(x) = m_A(x) - m_B(x)$ and $\delta_2(x) = m_A(x) - \alpha^{-1}m_B(\alpha x)$ are known functions obtained from measurements. Assume that the functions $\delta_1(x)$, $\delta_2(x)$, $\varepsilon_A(x)$ and $\varepsilon_B(x)$ can be expanded as a power series in a given domain $D = [x_1, x_2]$, that is,

$$\begin{aligned} &\delta_1(x) = \sum_{n=0}^{N} d_n^{(1)} x^n \text{ and } \delta_2(x) = \sum_{n=0}^{N} d_n^{(2)} x^n, \\ &\varepsilon_A(x) = \sum_{n=0}^{N} e_n^{(A)} x^n \text{ and } \varepsilon_B(x) = \sum_{n=0}^{N} e_n^{(B)} x^n. \end{aligned} \quad (27)$$

For a given set of data points of $\delta_1(x)$ and $\delta_2(x)$, the coefficients $d_n^{(1)}$ and $d_n^{(2)}$ can be obtained using the least-squares method. Except for n =1, the coefficients $e_n^{(A)}$ and $e_n^{(B)}$ can be determined by

$$e_n^{(A)} = \frac{d_n^{(2)} - \alpha^{n-1} d_n^{(1)}}{1-\alpha^{n-1}} \text{ and } e_n^{(B)} = \frac{d_n^{(2)} - d_n^{(1)}}{1-\alpha^{n-1}}. \quad (n = 0, 2, 3 \cdots N) \quad (28)$$

For n =1, since the functional equations (26) are reduced to one independent equation, there is only a single equation $d_1^{(1)} = d_1^{(2)} = e_1^{(A)} - e_1^{(B)}$ for two unknowns $e_1^{(A)}$ and $e_1^{(B)}$. To determine the remaining unknown coefficients $e_1^{(A)}$ and $e_1^{(B)}$, we use an integral expression

$$e_1^{(A)} = \frac{2}{x_{2s}^2 - x_{1s}^2} \int_{x_{1s}}^{x_{2s}} [m_A(x) - \sum_{\substack{n=0 \\ n\neq 1}}^{N} e_n^{(A)} x^n] dx - 1, \quad (29)$$

and the relation $e_1^{(B)} = e_1^{(A)} - d_1^{(1)}$. The given domain $D_s = [x_{1s}, x_{2s}]$ ($x_{1s}^2 \neq x_{2s}^2$) for integration is a sub-domain of the measurement domain $D = [x_1, x_2]$.

As discussed previously, since the true variable x is not known *a priori* in practical applications, approximation should be used in which the true variable x is replaced by the known approximate variable $m_A(x)$. The approximate formulations are

$$\begin{aligned} \delta_1(x)_{appr} &= \sum_{n=0}^{N} d_n^{(1)} [m_A(x)]^n, \\ \delta_2(x)_{appr} &= \sum_{n=0}^{N} d_n^{(2)} [m_A(x)]^n, \\ \varepsilon_A(x)_{appr} &= \sum_{n=0}^{N} e_n^{(A)} [m_A(x)]^n, \\ \varepsilon_B(x)_{appr} &= \sum_{n=0}^{N} e_n^{(B)} [m_A(x)]^n. \end{aligned} \quad (30)$$

where $\delta_1(x)_{appr} = m_A(x) - m_B(x)$ and $\delta_2(x)_{appr} = m_A(x) - \alpha^{-1} m_B(\alpha m_A(x))$ are known functions. The approximate bias errors $\varepsilon_A(x)_{appr}$ and $\varepsilon_B(x)_{appr}$ can be determined by using Eqs. (28) and (29). The approximations $\varepsilon_A(x)_{appr}$ and $\varepsilon_B(x)_{appr}$ describe the general behavior of the bias error distributions, but deviate from the true ones. The linear model for correcting $\varepsilon_A(x)_{appr}$ and $\varepsilon_B(x)_{appr}$ is given by

$$\varepsilon_A(x) = \varepsilon_A(x)_{appr} - [C_{A0} + C_{A1} m_A(x)]$$
$$\varepsilon_B(x) = \varepsilon_B(x)_{appr} - [C_{B0} + C_{B1} m_A(x)] . \quad (31)$$

When two true values are known at two specific points, the constants C_{A0}, C_{A1}, C_{B0}, and C_{B1} can be determined.

Simulations indicate that Eq. (31) is able to describe a class of the bias error distributions $\varepsilon_A(x)$ and $\varepsilon_B(x)$ that are reasonably represented by a power series. As an example, we consider the bias error distributions $\varepsilon_A(x)$ and $\varepsilon_B(x)$ in $D = [1,10]$

$$\varepsilon_A(x) = 0.3 - 4\times10^{-2}\sqrt{x} - 2\times10^{-4}x^2 - 8\times10^{-5}x^4 ,$$
$$\varepsilon_B(x) = 0.1 - 5\times10^{-3}\sqrt{x} + 2\times10^{-2}x^2 - 3\times10^{-4}x^3 . \quad (32)$$

Figure 9 shows the given and calculated bias error distributions $\varepsilon_A(x)$ and $\varepsilon_B(x)$ for α = 2 and N = 10. The empirical rule for selecting the order of the polynomials in Section 3 is also applicable to the two-device case.

The Translation-Based Method

In a domain $D_\theta = [0,2\pi]$, the intrinsic functional equations for the bias errors $\varepsilon_A(\theta)$ and $\varepsilon_B(\theta)$ are

$$\delta_1(\theta) = \varepsilon_A(\theta) - \varepsilon_B(\theta)$$
$$\delta_2(\theta) = \varepsilon_A(\theta) - \varepsilon_B(\theta + \theta_0) , \quad (33)$$

where θ_0 is a constant translation in radian, $\delta_1(\theta) = m_A(\theta) - m_B(\theta)$, and $\delta_2(\theta) = m_A(\theta) - m_B(\theta + \theta_0) + \theta_0$ are known functions. Assume that in $D_\theta = [0,2\pi]$ the functions $\delta_1(\theta)$, $\delta_2(\theta)$, $\varepsilon_A(\theta)$ and $\varepsilon_B(\theta)$ can be expanded as

$$\delta_1(\theta) = a_0^{(1)}/2 + \sum_{n=1}^{N} [a_n^{(1)} \cos(n\theta) + b_n^{(1)} \sin(n\theta)] ,$$
$$\delta_2(\theta) = a_0^{(2)}/2 + \sum_{n=1}^{N} [a_n^{(2)} \cos(n\theta) + b_n^{(2)} \sin(n\theta)] ,$$
$$\varepsilon_A(\theta) = a_0^{(A)}/2 + \sum_{n=1}^{N} [a_n^{(A)} \cos(n\theta) + b_n^{(A)} \sin(n\theta)] ,$$
$$\varepsilon_B(\theta) = a_0^{(B)}/2 + \sum_{n=1}^{N} [a_n^{(B)} \cos(n\theta) + b_n^{(B)} \sin(n\theta)] . \quad (34)$$

The coefficients ($a_n^{(1)}$, $b_n^{(1)}$, $a_n^{(2)}$, $b_n^{(2)}$) in $\delta_1(\theta)$ and $\delta_2(\theta)$ can be determined using the least-squares method. For $n \neq 0$, a relation between ($a_n^{(A)}$, $b_n^{(A)}$, $a_n^{(B)}$, $b_n^{(B)}$) and ($a_n^{(1)}$, $b_n^{(1)}$, $a_n^{(2)}$, $b_n^{(2)}$) is

$$\left(a_n^{(A)}\ b_n^{(A)}\ a_n^{(B)}\ b_n^{(B)}\right)^T = G^{-1}\left(a_n^{(1)}\ b_n^{(1)}\ a_n^{(2)}\ b_n^{(2)}\right)^T ,$$
$$(n = 1,2,3\cdots N) \quad (35)$$

where

$$G = \begin{pmatrix} 1 & 0 & -1 & 0 \\ 0 & 1 & 0 & -1 \\ 1 & 0 & -\cos(n\theta_0) & -\sin(n\theta_0) \\ 0 & 1 & \sin(n\theta_0) & -\cos(n\theta_0) \end{pmatrix} .$$

Since the determinant of G is $det(G) = 2[1 - \cos(n\theta_0)]$, a necessary condition for the existence of a unique solution is $n\theta_0 \neq k\pi + \pi/2$ ($k = 0,1,2,\cdots$). For $n = 0$, only one equation $a_0^{(1)} = a_0^{(2)} = a_0^{(A)} - a_0^{(B)}$ is available for two unknowns $a_0^{(A)}$ and $a_0^{(B)}$. Using a similar method to the pure scaling case, the coefficient $a_0^{(A)}$ can be determined by an integral over $D_\theta = [0,2\pi]$

$$a_0^{(A)} = \pi^{-1} \int_0^{2\pi} \{ m_A(\theta) - \sum_{n=1}^{N} [a_n^{(A)} \cos(n\theta) + b_n^{(A)} \sin(n\theta)] \} d\theta - 2\pi . \quad (36)$$

Therefore, the coefficient $a_0^{(B)} = a_0^{(A)} - a_0^{(1)}$ is readily known. As an example, we consider the following bias errors $\varepsilon_A(\theta)$ and $\varepsilon_B(\theta)$ in $D_\theta = [0,2\pi]$

$$\varepsilon_A(\theta) = 0.03 + 5\times10^{-4}\theta + 0.02\cos(\theta) + 3\times10^{-3}\cos(2\theta) - 6\times10^{-3}\sin(\theta) + 4\times10^{-4}\sin(3\theta)$$
$$\varepsilon_B(\theta) = 0.05 + 3\times10^{-4}\theta + 0.05\cos(\theta) - 6\times10^{-3}\cos(3\theta) + 10^{-4}\sin(\theta) + 3\times10^{-3}\sin(4\theta) \quad (37)$$

Figure 10 shows a comparison between the given bias errors and those computed by using the translation-based method ($\theta_0 = \pi/35$ and $N = 6$).

6. Applications

In principle, the aforementioned methods are applicable to any device. Here, to illustrate applications of these methods, we present several typical examples in voltage measurements, angular measurements, and optical measurements.

Voltage Calibrations for A/D Converter

A voltage divider was constructed using stable resistors to obtain a nominal voltage ratio of 0.5 (the scaling constant 0.5 in the scaling-based method). The

input to the voltage divider was connected to a stable voltage source and the output was connected to one channel of a 24 bit multiplexing A/D converter (Lawson Model 201). Another channel was connected directly to the voltage source. The voltage source was varied from –5v to +5v (the full range of the A/D converter). The 100 readings on both channels were recorded. No accuracy was assumed for the voltage source or the voltage divider ratio. Calculation for the bias error distribution was performed by using the approximate scaling-based method. Two reference readings were taken to provide the standard values, one with the input shorted and another with the input voltage set to exactly 3 volts (as measured on a precision voltmeter (HP 3458A) of the accuracy of 8ppm). This is all that is required to find the calibration of the A/D converter by using the approximate scaling-based method. Eleven additional points were taken using the precision voltmeter (HP 3458A) over the full range to verify the mathematical solution. The voltage calibration plots in Fig. 11 shows the verification points and the calibration results computed using the scaling-based method for α = 0.5 and N = 15. The calibration curve computed by using the scaling-based method is in good agreement with the verification data.

Instead of using a voltage divider for scaling, scaling can be achieved based on dial readings of a power supply (Wavetek Model 220). An advantage of this approach is that a physical device like the divider is no longer required for scaling. Figure 11 shows the bias error distribution computed by using the scaling-based method in which scaling is controlled based on the dial readings. Compared with the results given by using the divider, the distribution obtained by using the dial readings shows larger local variations. This is because the mechanical voltage setting device of the power supply caused abrupt voltage variations over a certain range of operation. It is expected that a more stable device will produce a smoother bias error distribution.

Angle Calibrations for Encoder and Indexing Table

The two-device translation-based method was used for angle calibration on a dividing head with attached encoder. The secondary device was an indexing table with a resolution of one degree. Both devices have a nominal accuracy specification of one arc second. The axis of rotation was horizontal so that a precision servo accelerometer was used as an indicator of level. The procedure involves rotating the dividing head clockwise in 10^o increments, rotating the indexer counter-clockwise in 10^o increments, and reading the level as indicated by the precision accelerometer. The second set of data, taken with the indexer and accelerometer translated -60 degrees. To recover the bias error distributions, the first set of data and the second set of -60^o-translated data were processed by using the two-device translation-based method with a 4th-order Fourier series. The calibration curves for both the encoder and indexing table can be simultaneously determined, as shown in Fig. 12. The black circular points in Fig. 12 are the results of a conventional calibration using a device with an accuracy four times better than the dividing head with the encoder. The bias error distribution measured by using the precision accelerometer is in good agreement with the computed distribution for the encoder. It is worthwhile noting that we do not explicitly use any standard value to recover the bias error distribution. Nevertheless, the periodicity condition $\theta(0) = \theta(2\pi)$, which is automatically satisfied in the Fourier series solution, can be considered as an imposed constraint. The two-device translation-based method, originally proposed by Finley [3], has been used regularly by Wyle Laboratories to calibrate precision angle-measuring devices in their facility and at NASA Langley.

Radial Lens Distortion

An interesting example is application of the scaling-based method to determination of the radial lens distortion. In reality, a lens used for imaging is not perfect and the imperfect lens may distort an image. Thus, camera calibration to determine the camera parameters including the lens distortion parameters is crucial for accurate image-based measurements [7]. The most dominant lens distortion is the radial lens distortion that is symmetric about the principal-point (close to the geometric center of an image). The radial lens distortion is described by a simple model $\delta r = K_1 r^3$, where δr is a bias error in the radial distance due to the lens distortion, K_1 is the radial distortion parameter, and r is the radial distance from the principal-point. The radial distortion parameter K_1 in addition to other camera parameters can be obtained in comprehensive camera calibrations by using analytical photogrammetric techniques. For an 8mm Computar TV lens used in this test, an optimization camera calibration method [7] gives $K_1 = 0.001297\, mm^{-2}$.

Unlike analytical photogrammetric techniques that use a special mathematical model for the lens distortion, the scaling-based method determines the radial lens distortion under a general theoretical framework of the bias error. During tests, a 22in×17in target plate with 121 retro-reflective targets of 1/2in diameter was used to provide a planar target field. A CCD video camera (Hitachi KP-F1U) with an 8mm Computar TV lens, viewing perpendicularly the target plate, was used to take images of the plate placed at two different distances from the camera. Figure 13 shows typical images of the target plate at two different distances from the camera. The digitized image has 640×480 pixels and the nominal pixel spacing is 9.9 μm in both the horizontal and vertical directions. The centroids of the targets and the radial distances of the targets from the geometric center in these images were computed. Two images of the target plate at two different distances from the camera naturally provide scaling in the radial distance in image plane. The scaling constant

$\alpha = 0.8262$ was obtained by averaging ratios between the radial distances of the corresponding targets from the geometric center in two images. The bias error distribution $\varepsilon(r)$ was calculated by using the approximate scaling-based method when the order of the polynomial is suitably chosen in N = 20-28. By the definition of $\varepsilon(r)$, one knows $\delta r(r) = -\varepsilon(r)$. The condition $\delta r(0) = 0$ must be satisfied. Thus, only one standard value is required to determine the unknown constants in Eq. (22), which is given by the optimization camera calibration method. Figure 14 shows the radial lens distortion distributions obtained by the scaling-based method (N = 25) and the optimization camera calibration method for an 8mm Computar TV lens.

7. Conclusions

The bias error distribution of a device can be sought as a solution of the intrinsic functional equation. Based on this idea, the scaling- and translation-based methods have been developed to determine the bias error distribution in a domain from less accurate measurements. The scaling-based method is applicable to a device whose bias error distribution can be adequately expressed as a power series or a polynomial in a domain. Practical application of the scaling-based method typically requires two standard values to recover the complete bias error distribution in the whole domain. The suitable order of a polynomial for accurate recovery of the bias error distribution can be selected according to an empirical rule proposed in this paper. The translation-based method, which uses a Fourier series to describe the bias error distribution, is particularly useful for angular measurements because of the internal periodicity constraint. The translation-based method does not explicitly require any standard value. These methods have been extended to simultaneously determine the bias error distributions for two devices. To validate and clarify the technical aspects of these methods, computational simulations have been carried out for various hypothetical distributions of the bias error. Laboratory tests have been conducted for calibrating several different devices such as A/D converter, angular measurement device and optical lens. These methods of estimating the bias error distribution are effective for a variety of devices.

References:

[1] Coleman, H. W. and Steele, W. G., Experimentation and uncertainty analysis for engineers, John Wiley & Sons, New York, 1989.

[2] Bevington, P. R. and Robinson, D. K., Data reduction and error analysis for the physical sciences, McGraw-Hill, Inc., New York, 1992.

[3] Finley, T. D., Technique for calibration angular measurement devices when calibration standards are unavailable, NASA Technical Memorandum 104148, August 1991.

[4] Snow, W. L., Comments regarding the modelling of bias error in certain angular measurement devices using Fourier techniques, NASA Technical Memorandum 109048, November 1993.

[5] Aczel, J., Lectures on functional equations and their applications, Volume 19 of Mathematics in Science and Engineering. Academic Press, 1966.

[6] Castillo, E. and Ruiz-Cobo, M. R., Functional equations and modelling in science and engineering, Volume 161 of Monographs and Textbooks in Pure and Applied Mathematics, Marcel Dekker, Inc., New York, 1992.

[7] Liu, T., Cattafesta, L. N., Radeztsky, R. H., and Burner, A. W., Photogrammetry applied to wind-tunnel testing, AIAA J., Vol. 38, No. 6, 2000, pp. 964-971.

Appendix: Least-Squares Estimation of the Coefficients

To determine the coefficients $d_n \ (n = 0,1,2,\cdots N)$ in the power series or polynomial $\delta(x)$ in Eq. (7) for a set of data points $x_i \ (i = 1,2,\cdots M)$, a system of equations for $d_n \ (n = 0,1,2,\cdots N)$ is

$$\boldsymbol{P}\,\boldsymbol{d} = \boldsymbol{\delta}, \tag{A1}$$

where $\boldsymbol{d} = \left(d_0 \ d_1 \ d_2 \cdots d_N\right)^T$,

$\boldsymbol{\delta} = \left(\delta(x_1) \ \delta(x_2) \cdots \delta(x_M)\right)^T$, and

$$\boldsymbol{P} = \begin{pmatrix} 1 & x_1 & x_1^2 & x_1^2 & \cdots & x_1^N \\ 1 & x_2 & x_2^2 & x_2^2 & \cdots & x_2^N \\ & & \vdots & & & \\ 1 & x_M & x_M^2 & x_M^2 & \cdots & x_M^N \end{pmatrix}.$$

The least-squares solution to (A1) is

$$\boldsymbol{d} = (\boldsymbol{P}^T\boldsymbol{P})^{-1}\boldsymbol{P}^T\boldsymbol{\delta}. \tag{A2}$$

Similarly, a system of equations for the coefficients ($a_n^{(\delta)}$, $b_n^{(\delta)}$) in the Fourier series in Eq. (14) for a set of data points $\theta_i \ (i = 1,2,\cdots M)$ is

$$\boldsymbol{F}\,\boldsymbol{a} = \boldsymbol{\delta}, \tag{A3}$$

where $\boldsymbol{a} = \left(a_1^{(\delta)} \cdots a_N^{(\delta)} \, b_1^{(\delta)} \cdots b_N^{(\delta)}\right)^T$,

$\boldsymbol{\delta} = \left(\delta(\theta_1) \ \delta(\theta_2) \cdots \delta(\theta_M)\right)^T$, and

$$\boldsymbol{F} = \begin{pmatrix} cos(\theta_1)\cdots cos(N\theta_1) & sin(\theta_1)\cdots sin(N\theta_1) \\ cos(\theta_2)\cdots cos(N\theta_2) & sin(\theta_2)\cdots sin(N\theta_2) \\ & \vdots \\ cos(\theta_M)\cdots cos(N\theta_M) & sin(\theta_M)\cdots sin(N\theta_M) \end{pmatrix}.$$

The least-squares solution to (A3) is

$$\boldsymbol{a} = (\boldsymbol{F}^T\boldsymbol{F})^{-1}\boldsymbol{F}^T\boldsymbol{\delta}. \tag{A4}$$

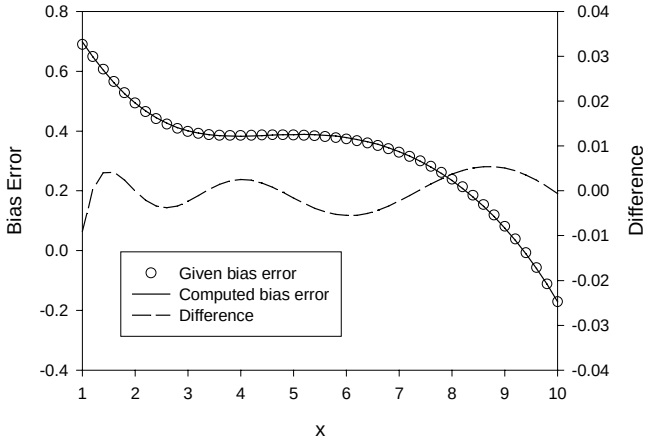

Fig. 1. The given bias error distribution and computed results by using the scaling-based method ($\alpha = 2$, $N = 13$).

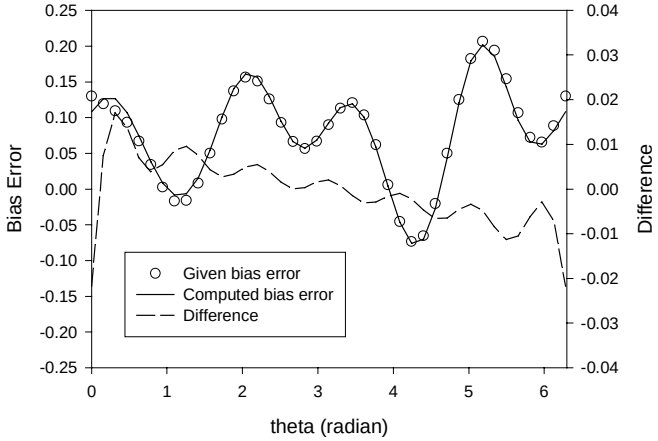

Fig. 2. The given bias error distribution and calculated results by using the translation-based method ($\theta_0 = \pi / 20$, $N = 6$).

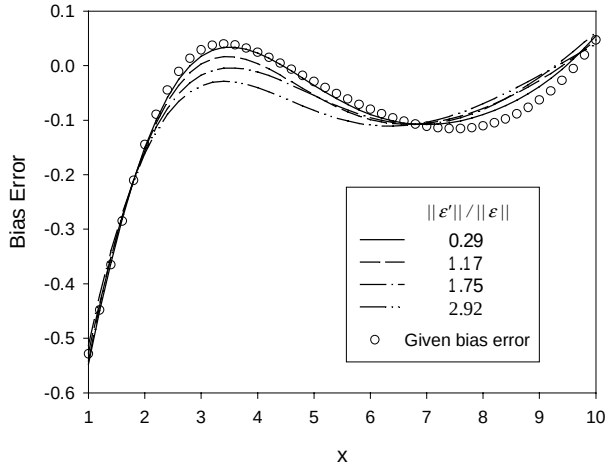

Fig. 3. The given bias error distribution and calculated results by using the approximate scaling-based method ($\alpha = 2$, $N = 13$) for four magnitudes of the bias error of the approximate reference value.

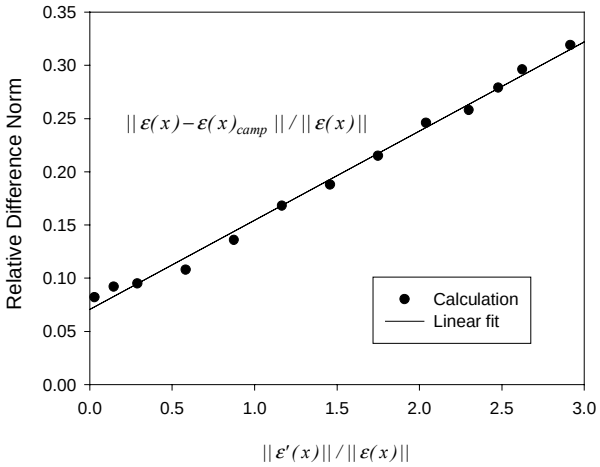

Fig. 4. The difference between the given and computed bias errors as a function of $||\varepsilon'(x)|| / ||\varepsilon(x)||$.

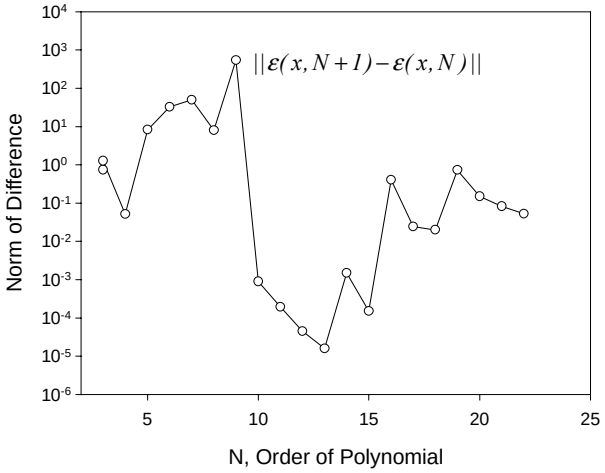

Fig.5. The difference norm $||\varepsilon(x,N+1)-\varepsilon(x,N)||$ as a function of the order of a polynomial N.

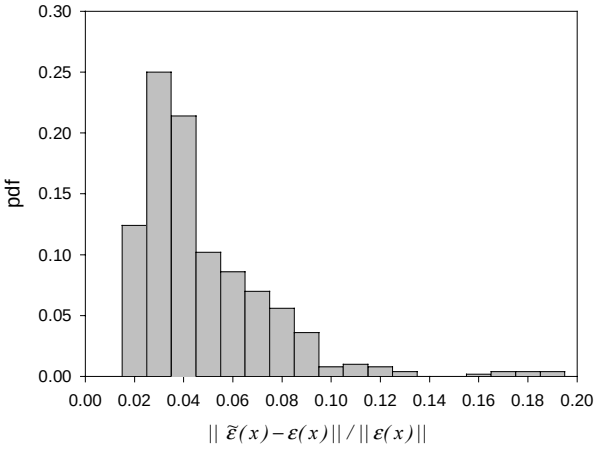

Fig. 6. The probability density function of $||\tilde{\varepsilon}(x)-\varepsilon(x)|| / ||\varepsilon(x)||$ for a randomly perturbed measurement.

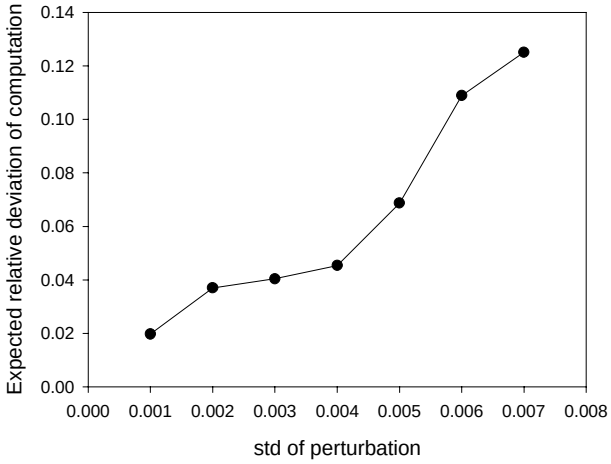

Fig.7. The expectation value of $|| \tilde{\varepsilon}(x) - \varepsilon(x) || / || \varepsilon(x) ||$ as a function of the standard deviation of the random perturbation.

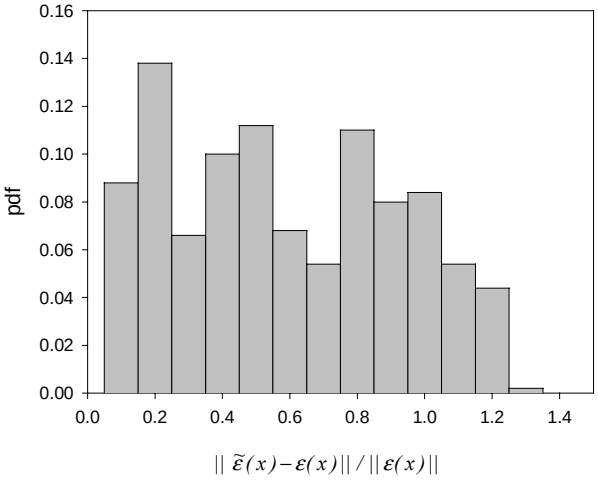

Fig. 8. The probability density function of $|| \tilde{\varepsilon}(x) - \varepsilon(x) || / || \varepsilon(x) ||$ for a randomly perturbed scaling constant.

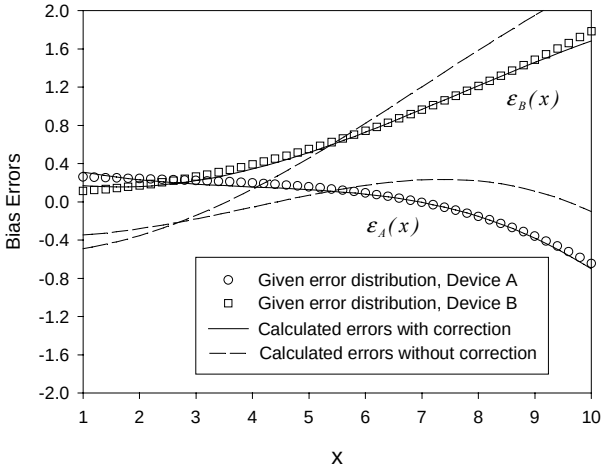

Fig. 9. The given bias error distributions and computed results by using the approximate two-device scaling-based method ($\alpha = 2$, $N = 10$) for devices A and B.

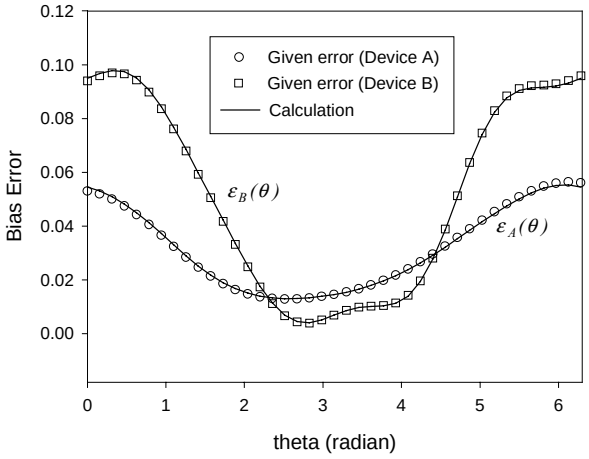

Fig. 10. The given bias error distributions and computed results by using the two-device translation-based method ($\theta_0 = \pi / 35$, $N = 6$) for devices A and B.

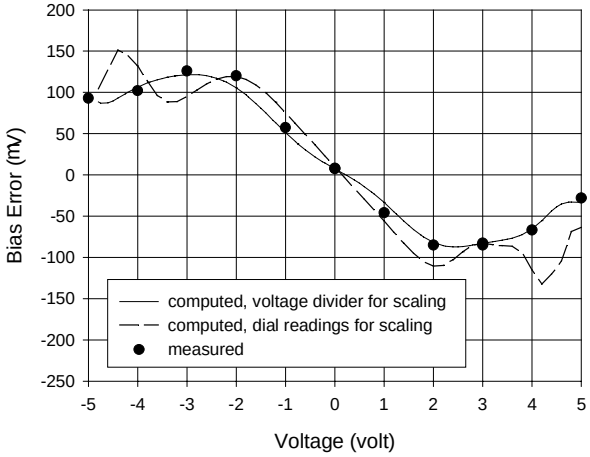

Fig. 11. The measured bias error distribution of voltage and computed results by using the scaling-based method ($\alpha = 0.5$, $N = 15$) for an A/D converter.

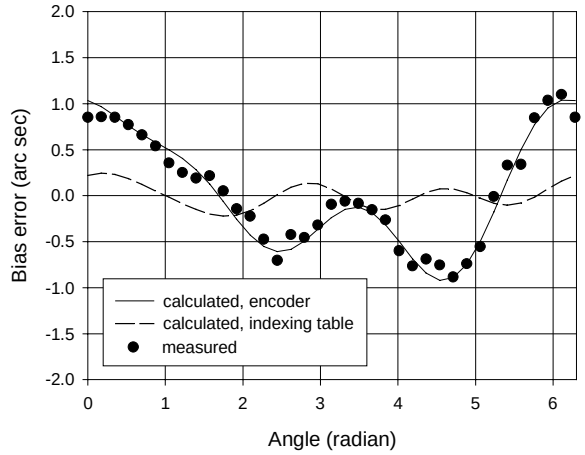

Fig. 12. The measured bias error distribution of angle and computed results by using the two-device translation-based method ($\theta_0 = -\pi / 3$, $N = 4$) for an encoder and an indexing table.

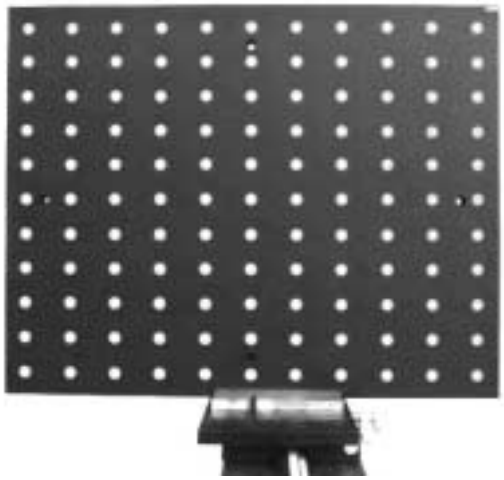

(a)

(b)

Fig. 13. Images of the target plate at two different distances relative to the camera.

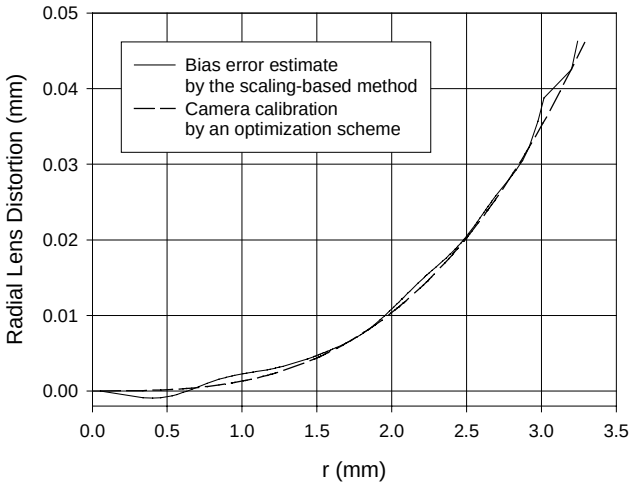

Fig. 14. The radial lens distortion distribution computed by using the scaling-based method ($\alpha = 0.8262$, $N = 25$) for of an 8mm Computar TV lens, along with the camera calibration result obtained by using an optimization method.